Meteorologische Zeitschrift, Vol. 13, No. 5, 373-379 (October 2004)

Article

Impact of street geometry on downward longwave radiation and air temperature in an urban environment

SIMONE BLANKENSTEIN* and WILHELM KUTTLER

Department of Applied Climatology and Landscape Ecology, University of Duisburg-Essen, Essen, Germany

(Manuscript received January 12, 2004; in revised form March 23, 2004; accepted March 29, 2004)

Abstract

A study on urban geometry has been carried out with regard to urban climate in a medium-sized central European city. Thereby the interrelation between the sky view factor (SVF, the portion of visible sky seen by an observer), downward longwave radiation and air temperature was analysed to get a closer look to the interaction of horizon obstructions, thermal radiation from urban surfaces and the urban heat island. Downward longwave flux and air temperature were measured by car traverses through the city of Krefeld, Germany, during clear and calm summer nights in 2003. The traverse included sections with buildings as well as sections with vegetation. Correlation of longwave radiation and SVF was close and negative with a coefficient of determination $R^2 = 0.91$, but urban heat island intensities (UHI, calculated from air temperature differences) along the route were weakly correlated with the SVF ($0.07 \leq R^2 \leq 0.39$). With buildings, UHI increased with a reduced SVF, but no tendency was found below trees. This was probably a main result from local topographic effects (cold air accumulation). The study indicates that a nocturnal urban heat island on a microscale is not only affected by horizon obstructions, but also by the spatially variable thermal properties of materials. Moreover, advection diminishes site specific air temperature differences even during low winds. On the other hand, longwave radiation strongly depends on geometric factors and can be predicted well with the SVF.

Zusammenfassung

Der Zusammenhang zwischen Straßenschluchtgeometrie und stadtklimatischen Eigenschaften wurde am Beispiel einer europäischen Mittelstadt untersucht. Dabei wurde die Beziehung zwischen Himmelssichtfaktor (SVF, dem Anteil des von einem Beobachter aus sichtbaren Himmels) und der abwärts gerichteten langwelligen Strahlung sowie der Lufttemperatur untersucht, um die Wechselwirkung zwischen Horizontüberhöhungen, Wärmeabstrahlung von Oberflächen und städtischer Wärmeinsel zu erfassen. Die Messungen von abwärts gerichteter langwelliger Strahlungsflussdichte und Lufttemperatur wurden mittels Messfahrten entlang einer festgelegten Route durch Krefeld (Deutschland) während klarer und überwiegend windschwacher Nächte im Sommer 2003 durchgeführt, wobei die Messroute sowohl bebaute Streckenabschnitte als auch Streckenabschnitte ausschließlich mit Vegetation umfasste. Während die Korrelation von langwelliger Strahlung und SVF sehr eng und negativ ausfiel ($R^2 = 0,91$), war die Beziehung zwischen der Wärmeinselintensität entlang der Messroute und dem SVF deutlich schwächer ($0,07 \leq R^2 \leq 0,39$). In Anwesenheit von Bebauung stieg die urbane Wärmeinselintensität (urban heat island, UHI) mit sinkendem SVF an. In einer ausschließlich durch Vegetation geprägten Umgebung konnte jedoch keine eindeutige Tendenz festgestellt werden, was überwiegend auf topographische Effekte (örtliche Kaltluftansammlung) zurückzuführen sein dürfte. Die Ergebnisse zeigen, dass die nächtliche urbane Wärmeinsel im mikroskaligen Bereich nicht streng dem jeweiligen SVF zugeordnet ist, da lokale Lufttemperaturunterschiede auch durch den räumlichen Wechsel der thermischen Untergrundeigenschaften bedingt sind sowie durch Advektion – auch bei schwachwindigen Wetterlagen – modifiziert werden. Dagegen ist die langwellige Strahlung stark an die geometrischen Verhältnisse gebunden, so dass der SVF ein geeignetes Vorhersagemaß für diese ist.

1 Introduction

Air temperature has been related to street geometry in several studies of urban climate (e.g. OKE, 1981; YAMASHITA et al., 1986; ELIASSON, 1996). Street geometry and longwave radiation have been intensively analysed by modelling and in case studies of single urban street canyons (ARNFIELD, 1982; VOOGT and OKE, 1991). But especially the role of urban street trees has not been taken into account so far and only few works realized in-situ measurements of street geometry and longwave radiation in more than one street canyon or in vegetation stands (NUNEZ and SANDER, 1981; NUNEZ et al., 2000). The characterization of urban geometry by means of the sky view factor (SVF) has become more feasible during the last years and calculation programs have been developed (HOLMER et al., 2001; CHAPMAN et al., 2001; GRIMMOND et al., 2001). Since nocturnal net longwave radiation is a forcing mechanism on urban energy balance, which in turn affects the nocturnal urban heat island (UHI), it is important to get

*Corresponding author: Simone Blankenstein, Department of Applied Climatology and Landscape Ecology, University of Duisburg-Essen, Campus Essen, Universitätsstraße 5, 45141 Essen, Germany, e-mail: simone.blankenstein@uni-essen.de

0941-2948/04/0013-0373 $ 3.15

DOI: 10.1127/0941-2948/2004/0013-0373

more knowledge about the spatial distribution of urban longwave radiation and air temperature in regard to urban geometry. The purpose of this study was to measure downward longwave radiation and air temperature patterns in various urban environments and relate them to the SVF to supplement the understanding of the thermal behaviour of cities and the interrelationship with their three-dimensional structure. Since the measurement of net longwave radiation (which means the additional measurement of upward longwave radiation from the ground) was not feasible with the mobile setup used here, only downward flux was recorded and net longwave radiation will not be discussed in this paper. Upward longwave flux is mainly a result from surface temperature. Downward longwave flux in street canyons results from surface temperature and also from surface geometries and surfaces sizes. Thus, it seems justified to measure downward longwave radiation only which seems to have the main impact on net radiation within street canyons.

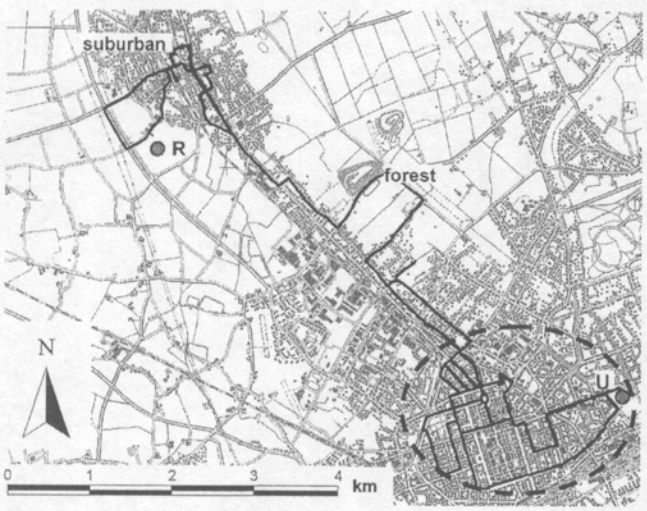

Figure 1: Overview of the study area in Krefeld. Solid line = route of vehicle traverses, dashed line = outline of the urban centre, R = rural reference station near a suburban area, U = start / end of vehicle traverses. The main part of the city extends to the east and south.

2 Methods

The study presented here was carried out in the city of Krefeld (238.000 inhabitants, 138 km^2, 51°20 N, 6°35 E), Germany, during June, July and August 2003. The city is located near the river Rhine, south-westerly of the Ruhr Basin and is surrounded by a rather ample rural environment. Elevations within the study area range from about 32 m a.s.l. to 39 a.s.l..

A 33.8 km long traverse across different urban environments was chosen. The route was divided into 205 sections with lengths from 40 m to 480 m. Depending on their character three categories were defined for the sections: a) built-up sections without vegetation, b) built-up sections with vegetation (e.g. with street trees in front of building walls) and c) sections with vegetation only. The route started and ended in the middle of a wide open space which is covered with asphalt and gravel near the city centre (U in Figure 1), led twice through a forest in a shallow basin and passed a rural reference station situated northwest of the urban centre (R in Figure 1). The rural site R is free of horizon obstructions (SVF = 1) and the urban site U is nearly free of horizon obstructions (SVF = 0.98, see also Figure 2 d)).

At the rural station R, global radiation (pyranometer type CM6B, Kipp & Zonen, 3.3 m a.g.l.), atmospheric counter radiation (L_R) (pyrgeometer type CG1, Kipp & Zonen, 3.3 m a.g.l.), wind speed, wind direction (cup anemometer type 4021 and vane type 4122, Th. Friedrichs, 4 m a.g.l.), air temperature and humidity (hygro-thermo transmitter, Thies, 2 m a.g.l.) were recorded automatically as means over three minutes. For mobile measurements of downward longwave radiation (L_{mobile}), another pyrgeometer (type CG1, Kipp & Zonen) was mounted horizontally on the top of a GPS-equipped van (3.3 m a.g.l.) and a Pt100 thermometer (Thies) was fit to the front (2 m a.g.l.). The CG1 pyrgeometer type was chosen since its response time is small (5 s) which was important for the mobile use of the sensor when driving through an environment with a large variety of SVF. Moreover the pyrgeometer has a field of view (FOV) of 150° instead of the ideal 180° FOV. This is relevant, when atmospheric counter radiation is measured although SVF is < 1 (i.e. that the sky is partly obstructed). With a 150° FOV, urban counter radiation at the urban site U could be quantified without obstruction influences to compare it with the rural counter radiation at R. It is important, to distinguish between atmospheric counter radiation L_R and downward longwave radiation L_{mobile} here: the first is the radiation from a sky without horizon obstructions, the latter is that from the visible part of the sky together with the radiation from horizon obstructions. Air constituents (NO, NO_2, O_3, CO, CO_2) were also sampled during the traverse to get information about specific air constituents of the urban and rural atmosphere.

Measurements were realized on seven clear and calm nights between 22:15 CET and 0:45 CET and lasted for about two hours. Speed of the measurement vehicle was maintained at 25 km h^{-1}. Data readings (sampling rate = 1 Hz) were averaged for each traverse section and were compared with the simultaneously recorded data at the reference station, after the sensors had been equalized. One traverse recorded about 7.200 data sets with 6 to 83 data sets per section (depending on section length).

Urban geometry of the traverse was specified with the sky view factor (SVF), which quantifies the visible sky at a certain location. It is a dimensionless parameter that ranges from zero (no sky visible) to unity

Table 1: Mean meteorological conditions at the rural reference site R during mobile measurements in Krefeld in summer 2003. t_a = air temperature, rH = relative humidity, L_R = counter radiation, v = wind speed, R = rural reference site. $\bar{x}$ = mean of all traverses, range = difference between maximum and minimum value.

Date	*time / CET*	$t_{a,R}$ / °C	rH_R / %	L_R / W m^{-2}	v_R / m s^{-1}	*prevailing wind direction*
13.06.2003	22:30–00:39	16.7	77	309	1.3	NNE
15.06.2003	22:30–00:36	16.3	76	307	1.0	N, NNW
24.06.2003	22:30–00:30	13.9	85	293	1.1	NNW
13.07.2003	22:51–01:06	17.8	66	320	2.2	ENE
31.07.2003	22:48–00:48	17.2	99	341	0.3	ESE
03.08.2003	22:27–00:18	19.3	84	345	0.8	NNE
05.08.2003	22:36–00:31	22.2	59	341	1.5	NE
$\bar{x}$		17.6	78	322	1.2	
range		8.3	40	52	1.9	

(no horizon obstructions visible). The advantage over other geometric measures like the height to width ratio H/W is that a complex environment can be considered much better (JOHNSON and WATSON, 1984). SVF along the measurement route were determined by use of fisheye imagery similar to the method of GRIMMOND et al. (2001). Photographs were taken on about every ten metres of the traverse with a digital camera (Coolpix 995 with fisheye converter FC–E8, Nikon) on the roof of a passenger car (1.6 m a.g.l.). The camera was operated with a remote cord (MC–EU1, Nikon) while the car was moving at walking speed. SVF were then calculated from the photographs with the Fortran program svf.exe (GRIMMOND et al., 2001). The numbers of photographs for each traverse section ranged from 5 to 55 depending on the section length. SVF were averaged for each traverse section so that one mean SVF could be attributed to each section.

3 Results and discussion

Date and mean meteorological conditions of the seven traverses are shown in Table 1. The sky was clear (< 2/8 cloud cover) during all mobile measurements. Mean wind speed reached up to 2.2 m s^{-1} and main wind direction had an east component in most cases. Atmospheric counter radiation at the rural reference station R ranged between 293 W m^{-2} and 345 W m^{-2} without marked changes during the two hours of the traverses. Relative humidity was 99 % (e = 19.4 hPa) in one case, but pyrgeometer temperature did not fall below dew point air temperature, thus the measurement of counter radiation was not disturbed by dew deposition onto the sensor.

3.1 Atmospheric counter radiation

Table 2 lists the mean differences between urban counter radiation L_U and rural counter radiation L_R during the start and end of the traverses. Mean $L_U - L_R$ was not more than 2 W m^{-2} and therefore can be neglected (because of measurement accuracy). The left column shows the corresponding air temperature differences between U and R, defined as mean $T_{a,U} - T_{a,R}$ at the start and end of the traverses. It is often reported that urban counter radiation exceeds that of rural areas due to vertical temperature structure and/or emissivity changes caused by air pollutants. For example, OKE and FUGGLE (1972) measured an increase of nocturnal urban counter radiation of 6.1 % in Montréal and TAPPER (1984) reported nocturnal urban counter radiation anomalies of 7.5 % for Christchurch in winter. ESTOURNEL et al. (1983) observed an increase of 5.4 % in Toulouse and NUNEZ et al. (2000) measured mean urban counter radiation excess of 3.6 % in Göteborg during summer.

The city of Krefeld is quite small and has lots of green spaces. Thus, $T_{a,U} - T_{a,R}$ was not very large ($\leq$ 2.1 K). Since concentrations of air constituents are generally low as one can see in Table 3, it can be presumed that aerosol concentration was small as well. Mean CO_2 concentration exceeded the natural background (376 ppm) about 21 ppm, but ESTOURNEL et al. (1983) computed that this amount has no measurable impact on urban counter radiation. If urban counter radiation excess $L_U - L_R$ is accepted as negligible in this study (0.6 % of L_R, see Table 2), then the spatial distribution of L_R can be assumed to be uniform over the study area during clear skies. This implicates, that spatial differences of longwave radiation measured on the traverse were mainly caused by horizon obstructions.

3.2 Sky view factors

Figure 2 demonstrates some exemplary photographs and corresponding SVF. The larger the SVF the more sky can be seen by an observer, and when vegetation is involved, the structures of sky and non-sky parts in the photographs are rich of details. The course of the SVF values along the route is visualized in Figure 3. The black squares symbolize the SVF section means whereas the variability of SVF within each section is depicted by grey points. In most cases SVF ranged from 0.6 to 0.8 (39.0 % of all sections) and from 0.8 to 1 (26.8 % of

Table 2: Urban heat island intensity ($T_{a,U} - T_{a,R}$) and urban counter radiation excess ($L_U - L_R$) in Krefeld during summer 2003. Values are means of measurements during the start and end of the traverses. R = rural reference site, U = urban reference site. $\bar{x}$ = mean of all traverses

date	*time / CET*	$T_{a,U} - T_{a,R}$ / K	L_R / W m^{-2}	$L_U - L_R$ / W m^{-2}	$\left(\frac{Lu-LR}{LR}\right) * 100$
13.06.2003	22:30–00:39	2.1	296	1	0.3
15.06.2003	22:30–00:36	1.3	293	3	1.0
24.06.2003	22:30–00:30	0.9	279	1	0.5
13.07.2003	22:51–01:06	1.3	302	2	0.5
31.07.2003	22:48–00:48	0.8	324	2	0.7
03.08.2003	22:27–00:18	2.0	325	4	1.3
05.08.2003	22:36–00:31	1.1	330	1	0.3
$\bar{x}$		1.3	307	2	0.6

Table 3: Air constituents measured on seven traverses (clear and calm nights) through the city of Krefeld in summer 2003. $\bar{x}$ = mean of all traverses, range = difference between maximum and minimum value.

date	*time / CET*	NO / $\mu g\ m^{-3}$	NO_2 / $\mu g\ m^{-3}$	O_3 / $\mu g\ m^{-3}$	CO / $\mu g\ m^{-3}$	CO_2 / *ppm*
13.06.2003	22:30–00:39	16	17	61	0	396
15.06.2003	22:30–00:36	11	12	13	0	401
24.06.2003	22:30–00:30	14	10	46	0	382
13.07.2003	22:51–01:06	5	8	1	0	369
31.07.2003	22:48–00:48	19	18	12	not meas.	442
03.08.2003	22:27–00:18	13	12	44	not meas.	392
05.08.2003	22:36–00:31	5	22	54	not meas.	397
$\bar{x}$		12	14	33	0	397
range		11	14	60	0	73

all sections). 17.1 % of the sections had SVF values between 0.4 and 0.6. Only 1 % of all sections were characterized by SVF smaller than 0.4. The reasons for large SVF ranges within the sections are as follows: When driving along a section, buildings and/or trees are seldom uniform. Their different heights and distances to the street as well as gaps between single buildings or tree crowns make the SVF variable on very short distances. Therefore SVF sections means consisted of a variety of very different SVF values.

3.3 Regressions of SVF, downward longwave radiation and UHI

Mean longwave radiation of each traverse section is denoted as Lmobile. The differences $L_{mobile} - L_R$ were averaged over all traverses and then correlated with the SVF of the corresponding traverse sections. The results in Figure 4 indicate strong interrelations ($R^2 = 0.91$) which can be well described with linear regressions. Since the slopes and intercepts of the regression lines are alike, the impact of vegetation on downward longwave flux on a horizontal surface was found to be similar to that of building walls. Since the sensor FOV and the measurement height of longwave radiation were different from the method of SVF determination, the solid regression lines in Figure 4 are shifted to smaller SVF values. However, L_{mobile}–L_R must be equal to zero when SVF = 1. Therefore, the regression line that would be expected is drawn as a dashed line in each diagram of Figure 4.

One can see from Figure 4 a) that the contribution of buildings to L_{mobile}–L_R is not larger than 48 W m^{-2}. Since SVF is small below dense canopies, trees increase the downward longwave flux to more then 70 W m^{-2} (see Figures 4 b) and c)).

The data scatter in case of Figures 4 b) and c) where vegetation contributes to the SVF is presumed to result from different reasons: On the one hand, SVF determination is difficult, when the photographs are rich of details, like it is the case with tree canopies. On the other hand, complex crown shapes with different distances to the ground as well as the complicated foliage geometry can cause data scatter when the sensor is moving below the canopy and the distances between sensor and surfaces vary strongly.

Figure 5 shows the interrelation of UHI and SVF analogously to the diagrams in Figure 4. Mean maximum heat island intensity ($UHI = T_{a,mobile} - T_{a,R}$) along the route was 2.7 K in the city centre and mean minimum heat island was – 1.6 K in the forest area because of cold air production. The correlation is much weaker than in the case of longwave radiation. The coefficient of determination is smallest in the built-up urban environment without vegetation ($R^2 = 0.07$, Figure 5 a)) and a positive UHI was observed at all locations. This could

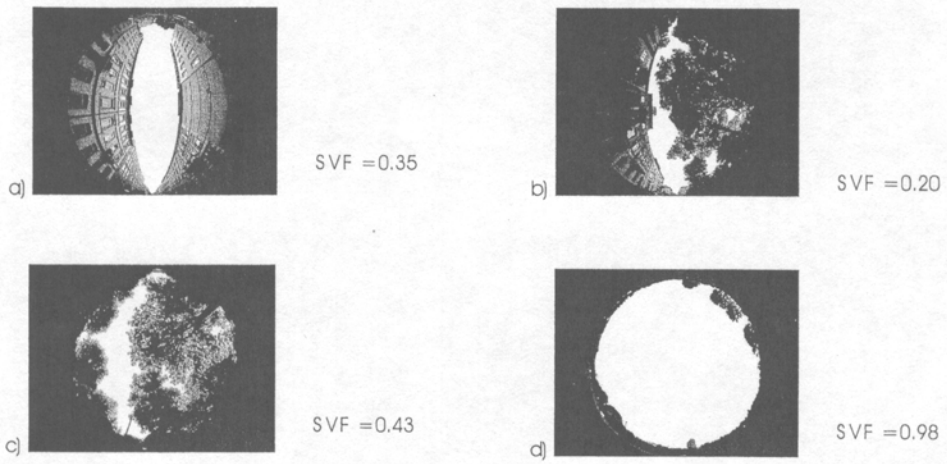

Figure 2: Examples of fisheye-photographs and SVF for three categories of street sections. The photographs are typical for a) built-up traverse sections without vegetation, b) built-up sections with vegetation, c) sections with vegetation only. Horizon obstructions at the urban reference site U are depicted in d).

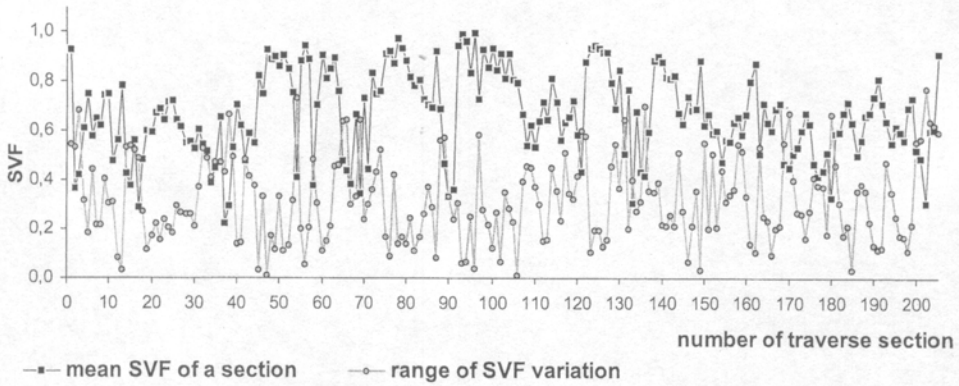

Figure 3: Course of SVF along a route through Krefeld in summer 2003. The city centre is represented by the sections no. 1 to 42 and no. 150 to 205. The rural reference station R was crossed at section no. 96. The range of SVF variation is the difference between SVF_{max} SVF_{min} within each single section.

result from the missing of very large and very small SVF values in this section category. In Figure 5 b) and c) one notices a contrast: Air temperature increases with decreasing SVF in case of a building vegetation mix along the route, because building blocks keep air temperatures high (Figure 5 b)). This is a consequence of net longwave radiation which varies with SVF and thermal properties of materials. In a pure vegetation environment, the upper site of the canopy cools down strongly and cold air sinks down to the ground. Then topography has an important role: In our case cold air accumulated in the forest stand (see Figure 1) which is situated about 4 m to 5 m lower than the surrounding area (A in Figure 5 c)). Additionally, cold air could have stemmed from a nearby hill (77 m a s.l.) in the north of the forest, thus could have strengthened the effect. Outside the forest, tree sections are closer to the built-up areas and are predominantly located a little bit higher, without cold air accumulation (B in Figure 5c)).

A weak interrelation of air temperature and SVF like it was observed in Krefeld was found in Göteborg by ELIASSON (1996): In five of six traverses, air temperature in 2 m and 0.2 m a.g.l. did not depend on SVF significantly. She stated that even sites of similar building density may show different air temperatures if the sites are located in different urban regions, because air temperature is governed by more complex factors then by the SVF alone and that advection, material properties, topographic effects and the location within the city (e.g. in the city centre or in a suburb) are responsible parameters. Further more, net radiation has an important role for the energy balance of street canyons. This means, that not only the downward radiation from obstructions (which was analysed in this study), but also the upward flux from the ground forces the air temperature pattern. YAMASHITA et al. (1986) determined a coefficient of determination $R^2 = 0.38$ for the statistical relationship between UHI and SVF. Matzarakis (2001) calculated a small interrelation ($R^2 = 0.14$) for yearly mean air temperature and SVF at different locations in Munich. Describing street geometry in terms of the median H/W of traverse sections in Singapore, GOH and CHANG (1999) found a similarly weak correlation ($R^2 = 0.28$). Instead, OKE (1981) stated a strong loga-

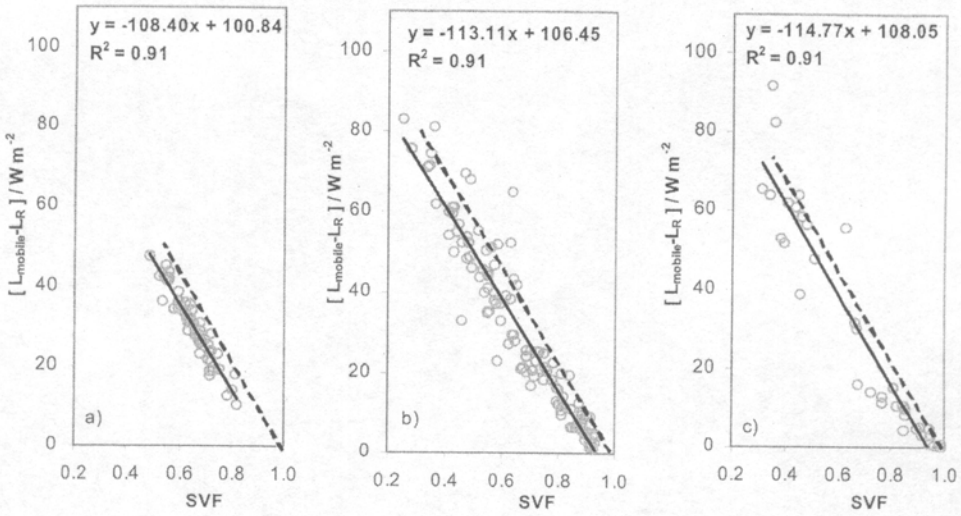

Figure 4: Plot of mean downward longwave radiation excess ($L_{mobile} - L_R$) versus sky view factors (SVF) along an urban-rural route. Each data pair represents the mean of seven nocturnal measurements in Krefeld during summer 2003: a) built-up traverse sections without vegetation, b) built-up sections with vegetation, c) sections with vegetation only. Dashed lines: Regression lines that would be expected if the measurement height and sensor FOV were identical with that of SVF determination. R^2 = coefficient of determination.

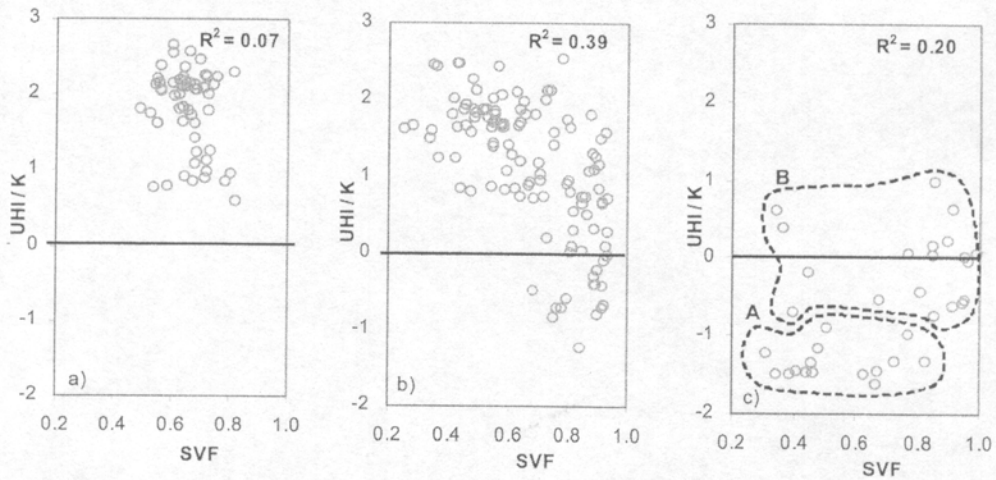

Figure 5: Plot of mean urban heat island UHI ($T_{a,mobile} - T_{a,R}$) versus sky view factors (SVF) along an urban-rural route. Each data pair represents the mean of seven nocturnal mobile measurements in Krefeld during summer 2003: a) built-up traverse sections without vegetation, b) built-up sections with vegetation, c) sections with vegetation only. A = sections with forest trees in a shallow basin. B = sections outside the forest stand. R^2 = coefficient of determination.

rithmic interrelation between UHI and H/W ($R^2 = 0.89$) and a strong linear relationship between UHI and SVF ($R^2 = 0.88$). But his study was based on a comparison between the centres of different cities, and each city centre region was characterized by a typical SVF. OKE (1981) pointed out, that the strong relationship must not be applied uncritically to other situations, e.g. to predict the spatial distribution of air temperature within a single city because this ignores the role of the spatially variable thermal admittance of surface and building materials. Moreover, SVF can be small at a certain location, e.g. under a tree, whereas the mean SVF of the whole area or district is rather large. Then air temperature will be characterized by the character of the area and not by the single SVF where the air temperature is measured. In opposite to air temperature, longwave radiation was found to depend closely on horizon obstructions of the surroundings. This is in accordance with NUNEZ et al. (2000) who calculated $0.90 \leq R^2 \leq 0.99$ in Göteborg by measuring downward longwave radiation at built-up streets and places with different SVF. Concerning vegetation, NUNEZ and SANDER (1981) noted $R^2 = 0.81$

when measuring longwave radiation balance at different SVF in an Eucalyptus forest in Tasmania.

4 Conclusions

A mobile method was used to detect the pattern of downward longwave flux and air temperature within street canyons and related the measurements to urban horizon obstructions. The results demonstrate that the interrelation between longwave radiation and SVF is very strong and similar for built-up and vegetation environments. However, air temperature is weakly correlated with street geometry because typical materials and building masses of urban regions are also important for air temperature. In addition, advection is almost always acting as a mixing term and the source area of a certain air volume can be located quite far away. Since the SVF does not describe surface properties and thermal inertia, it is concluded that air temperature distribution within a city can not be predicted well with SVF alone, but a tendency can be drawn from the results, at least in case of built-up areas. The mobile method used here was well satisfying to detect the spatial pattern of downward longwave radiation, even though the complex structure of plant canopies produces some data scatter.

5 Outlook

The results presented here convey information about horizon obstructions and longwave radiation for purposes of basic and applied research. They provide some empirical data material which could be used for validation of longwave radiation models and to extend those to non-infinite and non-symmetric street canyons. The study helps to understand the role of horizon obstructions concerning urban downward longwave radiation and its special impact on the urban heat island. Moreover, the results may serve as a mobile approach to get three-dimensional information about thermal radiation in cities, e.g. to expand the information from thermal imagery by remote sensing or to make up the balance of downward longwave fluxes for urban areas. These questions are investigated in the current works of a doctoral thesis.

Acknowledgements

The authors cordially thank Professor Sue GRIMMOND, Atmospheric Science Program Geography, Indiana University, Indiana, USA, for providing the program svf.exe and for helpful discussions.

References

ARNFIELD, A. J., 1982: An approach to the estimation of the surface radiative properties and radiation budgets of cities. – Phys. Geography **3**, 97–122.

CHAPMAN, L., J.E. THORNES, A.V. BRADLEY, 2001: Rapid determination of canyon geometry parameters for use in surface radiation budgets. – Theor. Appl. Climatol. **69**, 81–91.

ELIASSON, I., 1996: Urban nocturnal temperature, street geometry and land use. – Atmos. Environ. **30**, 379–392.

ESTOURNEL, C., R. VEHIL, D. GUEDALIA, J. FONTAN, A. DRUILHET, 1983: Observations and modelling of downward radiative fluxes (solar and infrared) in urban/ rural areas. – J. Clim. Appl. Meteorol. **22**, 134–142.

GOH, K.C., C.H. CHANG, 1999: The relationship between height to width ration and the heat island intensity at 22:00 h for Singapore. – Int. J. Clim. **19**, 1011–1023.

GRIMMOND, C.S.B., S.K. POTTER, H.N. ZUTTER, C. SOUCH, 2001: Rapid methods to estimate sky-view factors applied to urban areas. – Int. J. Clim. **21**, 903–913.

HOLMER, B., U. POSTGARD, M. ERIKSSON, 2001: Sky view factors in forest canopy calculated with IDRISI. – Theor. Appl. Climatol. **68**, 33–40.

JOHNSON, G.T., I.D. WATSON, 1984: The determination of view-factors in urban canyons. – J. Clim. Appl. Meteorol. **23**, 329–335.

MATZARAKIS, A., 2001: Die thermische Komponente des Stadtklimas. – Berichte des Meteorologischen Institutes der Universität Freiburg **6**, 267 pp.

NUNEZ, M., M. SANDER, 1981: Protection from cold stress in an eucalyptus shelterwood. – J. Climatol. **2**, 141–146.

NUNEZ, M., I. ELIASSON, J. LINDGREN, 2000: Spatial variations of incoming longwave radiation in Göteborg, Sweden. – Theor. Appl. Climatol. **67**, 181–192.

OKE, T.R., 1981: Canyon geometry and nocturnal heat island: Comparison of scale model and field observations. – J. Climatol. **11**, 237–254.

OKE, T.R., R.F. FUGGLE, 1972: Comparison of urban/rural counter radiation and net radiation at night. – Bound.-Layer Meteor. **2**, 290–308.

TAPPER, N., 1984: Prediction of the downward flux of atmospheric radiation in a polluted urban environment. – Aust. Meteor. Mag. **32**, 83–93.

VOOGT, J.A., T.R. OKE, 1991: Validation of an urban canyon radiation model for nocturnal long-wave fluxes. – Bound.-Layer Meteor. **54**, 347–361.

YAMASHITA, S., K. SEKINE, M. SHODA, K. YAMASHITA, Y. HARA, 1986: On the relationship between heat island and sky view factor in the cities of Tama river basin, Japan. – Atmos. Environ. **20**, 681–686.